MONK11A: STATUS AND PLANS FOR THE MONK MONTE CARLO CODE FOR CRITICALITY SAFETY AND REACTOR PHYSICS ANALYSES

S. D. Richards, G. P. Dobson, D. Hanlon, R. J. Perry, F. Tantillo and T. C. Ware
ANSWERS Software Service, Wood
Kings Point House, Queen Mother Square, Poundbury, Dorchester, United Kingdom, DT1 3BW

simon.richards@woodplc.com

ABSTRACT

Recent developments to the MONK® Monte Carlo code include, but are not limited to: improved physical modelling of bound thermal scattering and scattering at epithermal resonances; thermal power flux normalization and power distribution; continuous energy adjoint flux and kinetics parameters estimation; and improvements to the geometry modelling package and user input. Improvements to the nuclear data libraries to include the latest evaluations and bound thermal scattering for low temperature water and ice and other nuclides.

KEYWORDS: Monte Carlo, criticality, reactor physics

1. INTRODUCTION

MONK® is an advanced Monte Carlo neutronics code for the solution of criticality safety and reactor physics problems. It has a proven track record of application to the whole of the nuclear fuel cycle and is well established in the UK criticality community. Furthermore it is increasingly being used for reactor physics applications.

The current version of MONK is MONK10B which was released in 2017 after an extensive programme of enhancements over the previous versions [1,2]. This paper discusses the further significant developments which have been carried out since that release, and which will be incorporated into a forthcoming MONK11A release.

2. NEW AND IMPROVED FEATURES

2.1. Input Enhancements

The MONK input is free format, keyword driven and easy to read. It has powerful features for defining and using parameters, evaluating algebraic formulae, and looping over parameters with lists of values allowing sophisticated multivariate parameter surveys to be carried out from a single input.

2.1.1. Atomic mass parameters

Often the atomic masses of isotopes and elements are needed when defining material compositions using input formulae. To aid model QA and improve user convenience special atomic mass parameters have been provided to allow the atomic mass data in the material database file to be accessed from within the MONK input file.

2.2. Geometry Enhancements

The MONK geometry package comprises three components: *Fractal Geometry* (FG) which defines volumes of homogeneous materials as unions and intersections of simple geometric bodies; *Hole Geometry* (HG) which uses Woodcock tracking [3] and simplifies the specification of heterogeneous configurations in the volumes of space defined in FG; and CAD import. Each MONK release enhances these elements with new and improved capabilities.

2.2.1. Improved Random Hole

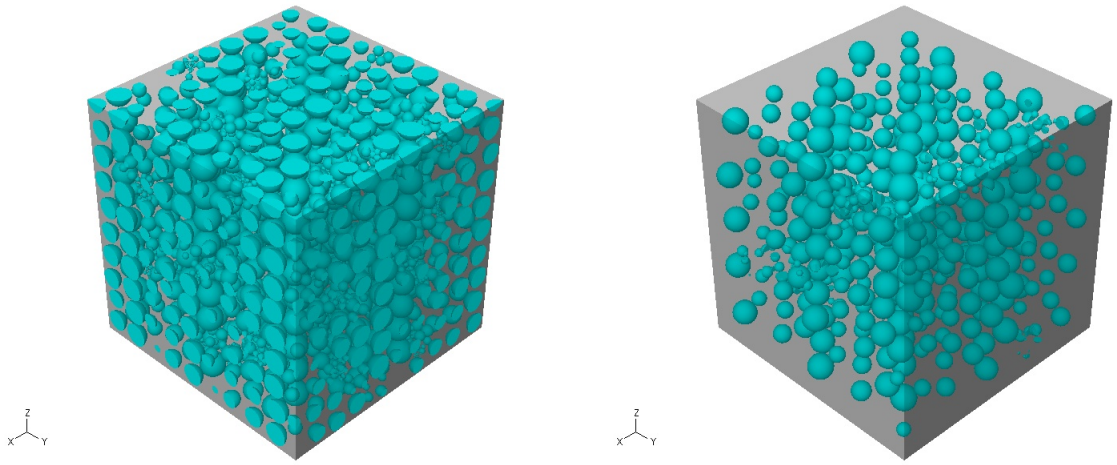

Figure 1: Examples of the Random Hole for modelling pseudo-random arrangements of spheres: original packing structure (left) and new packing structure with truncated spheres removed (right).

One of the Hole Geometry options is the Random Hole, which models a pseudo-random arrangement of spheres with a pseudo-random distribution of sizes. It is one of several Hole geometries in MONK which are stochastic in nature, but this one is unique in handling the random nature of the medium in real time during the Monte Carlo tracking rather than preprocessing the geometry at the start of the calculation. Enhancements to this capability for MONK11A address some of the limitations of the current approach by including: an increased packing fraction limit; an alternative arrangement of spheres which demonstrably reduces streaming planes; options for the user to influence the random number generation should the arrangement of spheres appear non-random; and the ability to influence the realism of the model by being able to prevent the truncation of spheres at the boundary of the containing volume.

2.3. Physics Enhancements

2.3.1. Bound thermal scattering data interpolation

For neutrons with energies below a few eV, the thermal motions of scattering nuclides profoundly affect the outcome of collisions. There are three important processes that occur here:

1. inelastic thermal scatter – a colliding neutron may either gain or lose energy from the motions of a bound target nucleus and some of the kinetic energy may be transferred to excited molecular quantum levels, e.g. rotation, vibration;
2. incoherent elastic scatter – the wave-like behaviour of the neutron combined with the random nature of some scattering media gives rise to incoherent elastic scatter where the neutron is scattered without change of energy. The angular distribution of the scattered neutrons is forward peaked and continuous; and
3. coherent elastic scatter – if the nuclei of the scattering medium are arranged in a well-defined array (i.e. a crystalline material) then coherent elastic scatter may occur. Scattering takes place into well-defined directions that are a function of the wavelength of the incident neutron and the lattice parameters.

For the inelastic thermal scattering, the cross-sections are given through the use of an $S(\alpha, \beta)$ function that is obtained from the analysis of the collisions using quantum mechanics. The data describing the $S(\alpha, \beta)$ function for a set of pre-determined temperatures are available in the form of evaluated nuclear data files. This type of scatter is especially important for bound hydrogen, and MONK currently uses these data for hydrogen in water, hydrogen in polythene and hydrogen in zirconium hydride, as well as for deuterium in D_2O, carbon in graphite, and beryllium and oxygen in BeO. Additionally, for the ENDF/B-VII.x libraries, these data are used for zirconium in zirconium hydride and silicon and oxygen in silicon dioxide (ENDF/B-VII.1 only).

MONK also treats incoherent elastic scatter for hydrogen in polythene, hydrogen in zirconium hydride and, for ENDF/B-VII, zirconium in zirconium hydride. This type of scattering is negligible for hydrogen in water. Coherent elastic scatter data are present for graphite, beryllium metal and beryllium oxide. Thermal scattering in all other nuclides is treated by applying a monatomic free-gas model. Even for bound nuclei, the monatomic gas model is applied when the incident energy is well in excess of the energy levels for internal oscillations.

In the BINGO collision processor in MONK any material may be set to any temperature T_{BROAD} above the base temperature of the BINGO library (this was 293.6 K for previous BINGO libraries but has been extended to lower temperatures for the latest libraries). If T_{BROAD} is within 0.5 K of a BINGO library temperature then the Doppler broadened nuclear cross-sections are obtained directly from the library file, otherwise run-time Doppler broadening is employed to determine the Doppler broadened cross-section at temperature T_{BROAD}.

The $S(\alpha, \beta)$ data needed to calculate secondary parameters for bound thermal scattering are stored in the BINGO library at a small number of fixed temperatures as shown in Table 1, and there is no straightforward way of interpolating these data analytically. The ENDF-6 Formats Manual [4]

states that "Experience has shown that temperature interpolation of $S(\alpha, \beta)$ data is unreliable. It is recommended that cross-sections be computed for the given moderator temperatures only. Data for other temperatures should be obtained by interpolation between the cross-sections." This recommendation is followed in the BINGO collision processor and the incoherent inelastic scattering cross-section is interpolated between the temperatures at which the $S(\alpha, \beta)$ data are given. However, this simple interpolation is not applicable to the calculation of secondary energy and angle, and the BINGO collision processor therefore uses the $S(\alpha, \beta)$ data at the closest tabulated temperature. In certain cases this can result in a significant change in reactivity for a small change in temperature, particularly where the temperature is near the midpoint between one $S(\alpha, \beta)$ temperature and the next. To address this issue a stochastic interpolation method has been implemented which randomly selects one of the bounding temperatures at each collision with probability determined by where the actual temperature lies in the range.

Nuclide	**JEFF-3.x and CENDL-3.1**	**ENDF/B-VII.x**
H in H_2O	293.6, 323.6, 373.6, 423.6, 473.6, 523.6, 573.6, 623.6, 647.2, 800.0, 1000.0	293.6, 350.0, 400.0, 450.0, 500.0, 550.0, 600.0, 650.0, 800.0
H in CH_2	293.6, 350.0	296.0 350.0
H in ZrH	293.6, 400.0, 500.0, 600.0, 700.0, 800.0, 1000.0, 1200.0	296.0, 400.0, 500.0 600.0, 700.0, 800.0 1000.0, 1200.0
D in D_2O	293.6, 323.6, 373.6, 423.6, 473.6, 523.6, 573.6, 643.9	293.6, 350.0, 400.0, 450.0, 500.0, 550.0, 600.0, 650.0
C in graphite	293.6, 400.0, 500.0, 600.0, 700.0, 800.0, 1000.0, 1200.0, 1600.0, 2000.0, 3000.0	296.0 400.0, 500.0, 600.0, 700.0, 800.0, 1000.0, 1200.0, 1600.0, 2000.0
Be and O in BeO	296.6, 400.0, 500.0, 600.0, 700.0, 800.0, 1000.0, 1200.0	296.6, 400.0, 500.0, 600.0, 700.0, 800.0, 1000.0, 1200.0
Be in Be metal	296.0, 400.0, 500.0, 600.0, 700.0, 800.0, 1000.0, 1200.0	296.0, 400.0, 500.0, 600.0, 700.0, 800.0, 1000.0, 1200.0
Z in ZrH	Not available	296.0 400.0, 500.0, 600.0, 700.0, 800.0, 1000.0, 1200.0
Si and O in SiO_2	Not available	293.6, 350.0, 400.0, 500.0, 800.0, 1000.0, 1200.0

Table 1: Temperatures (K) at which $S(\alpha, \beta)$ data are tabulated in the BINGO libraries.

The effect of the stochastic interpolation method is demonstrated in an example pincell model, consisting of a single 3.82 wt% enriched UO_2 unclad fuel rod of radius 0.48 cm, in the centre of a water-filled box with x and y dimensions of 1.2 cm. Reflecting boundary conditions are applied on all faces to represent an infinite array of fuel rods with a pitch of 1.2 cm. The hydrogen is modelled as ^{1}H bound in water and the oxygen is modelled as ^{16}O.

The fuel temperature in this model is fixed at 500.0 K and the water temperature is varied between 293.6 K (the base temperature of a standard BINGO library) and 1100.0 K (which is greater than the maximum $S(\alpha, \beta)$ tabulated temperature for water in the BINGO library used. Calculations are performed at each of the eleven tabulated temperatures and additionally at points 0.1 K above and below the midpoints between each library temperature in order to demonstrate the step change in k_∞ at the midpoints. A final point at 1100.0 K is used to demonstrate the behaviour at temperatures above the maximum $S(\alpha, \beta)$ tabulated temperature. A corresponding point below the minimum temperature of 293.6 K is not permitted since it is below the base temperature of the BINGO library. It is important to note that the water density is kept fixed at 0.99 g/cc for all temperatures in this test to allow the effect of the bound thermal scattering model to be decoupled from any

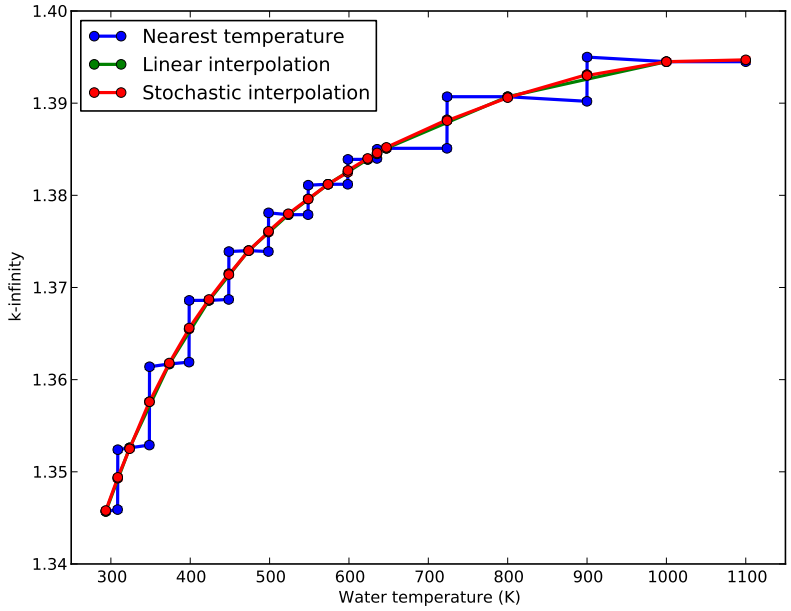

T (K)	k_∞		Δk (pcm)
	Nearest	Stochastic	
308.5	1.3459	1.3493	-340.0
308.7	1.3524	1.3494	+300.0
348.5	1.3529	1.3576	-470.0
348.7	1.3614	1.3576	+380.0
398.5	1.3619	1.3655	-360.0
398.7	1.3686	1.3656	+300.0
448.5	1.3687	1.3715	-280.0
448.7	1.3739	1.3714	+250.0
498.5	1.3739	1.3760	-210.0
498.7	1.3781	1.3761	+200.0
548.5	1.3779	1.3796	-170.0
548.7	1.3811	1.3796	+150.0
598.5	1.3812	1.3825	-130.0
598.7	1.3839	1.3827	+120.0
635.3	1.3840	1.3845	-50.0
635.5	1.3850	1.3846	+40.0
723.5	1.3851	1.3882	-310.0
723.7	1.3907	1.3881	+260.0
899.9	1.3902	1.3931	-290.0
900.1	1.3950	1.3930	+200.0

Figure 2: Comparisons between the results of the pincell calculation using the standard nearest temperature approach and the stochastic interpolation method. The standard deviation on the Monte Carlo results is 0.0001 (10 pcm).

effects of changing moderator density. All MONK calculations were run with a target standard deviation of 0.0001 using the JEFF-3.2 BINGO library.

The results of these calculations are plotted in Figure 2, which clearly shows the step changes which occur at the midpoints between the library temperatures when the code switches from the data tabulated at the lower temperature to the data tabulated at the higher temperature. Using the stochastic mixing approach eliminates these step changes, producing a smooth curve which passes through the midpoints of the step changes. Also shown in this figure is a linear interpolation, produced by post-processing results obtained at adjacent library temperatures to find the interpolated results at intermediate temperatures. The stochastic interpolation curve agrees very well with this interpolated curve (and largely overlies it as a result), but requires only a single calculation for each intermediate temperature and no post-processing. The table shows the degree to which the nearest temperature approach under predicts compared to the stochastic interpolation method at temperatures just below the midpoint between two tabulated temperatures, and over predicts at temperatures just above the midpoint.

2.3.2. Doppler broadening rejection correction (DBRC)

The DBRC method was implemented in MONK10B to improve the scattering kernel near epithermal resonances, requiring the elastic scattering cross-section at 0 K to be read from an external file. MONK11A will read these data directly from a compatible BINGO nuclear data library.

2.3.3. Thermal power neutron flux normalization and power distribution

The neutron flux can be now normalized to a given thermal power, using a factor calculated as [5]:

$$F = \frac{P\bar{\nu}}{1.6022 \cdot 10^{-13}\overline{Q^{\text{eff}}}}, \tag{1}$$

where P is the power, $\bar{\nu}$ is the average number of neutrons per fission and $\overline{Q^{\text{eff}}}$ is the average recoverable energy [†].

A further development allows the power distribution to be calculated in a user-defined mesh overlaid on the geometry with a user-defined energy group scheme. For each neutron that undergoes a fission reaction in a specific mesh, the following contribution is stored: $w\rho_i^j Q_i^{\text{eff}}$, where w is the neutron weight, ρ_i^j is the number density for isotope i contained in material j and Q_i^{eff} is the average recoverable energy for isotope i. At the end of the calculation all the contributions are normalized to the total reactor power.

2.3.4. IFP Adjoint flux and kinetics parameters estimators

A continuous energy adjoint flux estimator has been implemented in MONK based on the iterated fission probability (IFP) method. This uses the relationship between the neutron importance and the adjoint flux to derive an adjoint flux from a forward calculation. The methodology is extended to the estimation of kinetics parameters β_{eff} and neutron generation lifetime.

An accurate calculation of the kinetics parameters often implies the detailed knowledge of the so-called importance function, or adjoint flux, the calculation of which has been a formidable task for continuous energy Monte Carlo codes. In recent years, some authors have developed alternative ways to calculate kinetics parameters without the use of the adjoint function. Although the results are generally good, one of the main drivers of the current work was the possibility of using continuous energy Monte Carlo MONK calculations to estimate biases in deterministic codes, and this can only be done using the same weighting function in both codes.

The adjoint flux is also essential for sensitivity calculations; it allows the implementation of an exact perturbation theory, where absolute uncertainties evolve as a function of the perturbation amplitude. This is in contrast with the small perturbation hypothesis that limits the application of the correlated sampling and the differential operator methods.

If a neutron is inserted in a critical system, the neutron population will increase depending on the location $\mathbf{r}$, energy E and direction $\mathbf{\Omega}$ of the initial neutron. The importance of this neutron can then be thought of as proportional to the increase in reactor power, or anything related to it (e.g. fission neutrons, number of fissions and fission energy release), after a sufficient length of time has passed for the neutron population to converge to its asymptotic, or fundamental, shape [6].

[†] The average recoverable energy is the total energy released in the fission reaction minus the energy of the neutrinos, which is not deposited in the reactor.

Within the IFP framework, the asymptotic population is proportional to the importance of the ancestor neutron that started the chain, that is $\psi^*(\mathbf{r}, E, \mathbf{\Omega})$. The method is based on tallying, in the last generation, the number of neutrons produced by each neutron source in the first generation [7].

The IFP approach can be seen as an extension of the next fission probability (NFP) as a measure of the importance of a source neutron. In the NFP case, the importance is proportional to the number of neutrons produced in the next fission, while in the IFP case the importance is proportional to the progeny of an ancestor neutron after an arbitrary number of generations. While the NFP method yields similar results to the IFP method, the proportionality to the adjoint flux has only been proven for the latter.

Mathematically, the importance function in a particular point of the phase space can be expressed as [7]:

$$\psi^*(\theta_0) = k_{\theta_0}^{(1)} k_{\theta_0}^{(2)} ... k_{\theta_0}^{(\lambda-1)} k_{\theta_0}^{(\lambda)} k_{\text{eff}}, \tag{2}$$

where $\psi^*(\theta_0)$ represents the importance function in the phase space θ_0 and $k_{\theta_0}^{(i)}$ represents the multiplication factor that arises from a single source neutron, with θ_0 phase space coordinates, in the i-th generation. Assuming that the asymptotic population is reached after λ generations, the following multiplication factor will be equal to effective multiplication factor of the system.

Another equivalent mathematical definition, more suitable for the IFP implementation in MONK, makes use of the neutron population concept [8]:

$$\frac{\psi^*(\theta_1)}{\psi^*(\theta_2)} = \frac{N(\theta_1)}{N(\theta_2)}. \tag{3}$$

In this case, $N(\theta_k)$ represents the neutron population that arises from a single ancestor neutron with θ_k phase space coordinates, assuming the fundamental mode has been reached for the neutrons that started at θ_1 and θ_2.

Figure 3 shows results of MONK and WIMS calculations of the adjoint flux in the critical system TOPSY (HEU-MET-FAST-002) [9]. This system comprises a highly enriched uranium sphere surrounded by a thick reflector of natural uranium. Because of limitations in the WIMSECCO module used to model this system in WIMS it has been "cylinderized" using the average chord length equivalence:

$$\left(\frac{4}{3}\right) R_{\text{sphere}} = 2R_{\text{cylinder}} \tag{4}$$

The MONK calculation was performed using continuous energy Monte Carlo collision processing, with the adjoint flux being tallied in the WIMS 172 energy group scheme for direct comparison with the WIMS calculation. Adjoint flux spectra are plotted for both the fuel and reflector regions, and the radial dependence of the adjoint flux is shown in one fast energy group and one thermal

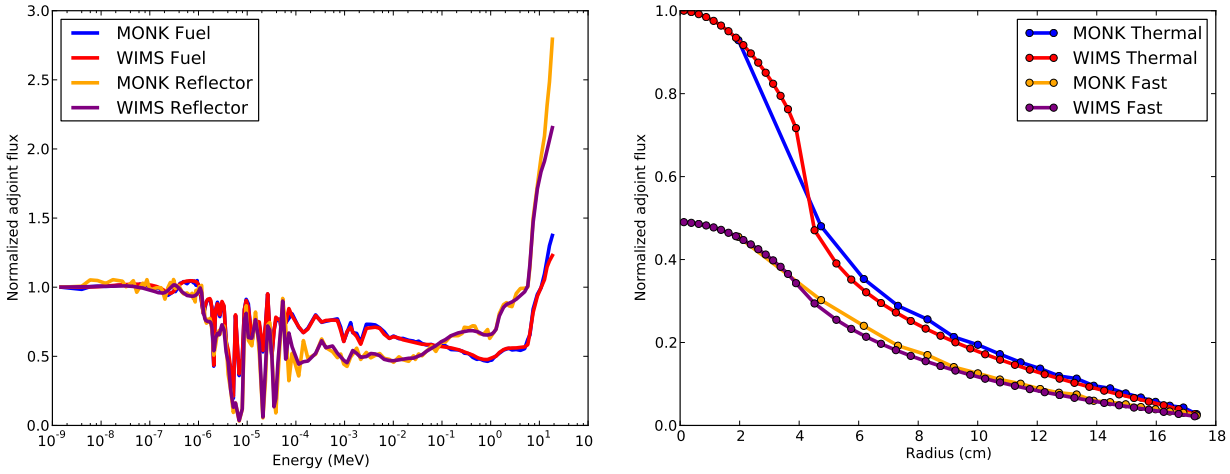

Figure 3: Comparison between MONK and WIMS calculations of the adjoint flux in the TOPSY benchmark, showing the adjoint flux spectrum in the fuel and reflector (left) and the radial adjoint flux distribution in one fast and one thermal group (right).

energy group (each of these represents a single energy group in the WIMS 172 group scheme, not a condensation of multiple fast and thermal groups). These results demonstrate generally good agreement between the two methods.

2.3.5. Improved fixed source capability

MONK is primarily used to solve eigenvalue problems, but can also be used to solve fixed source problems both using continuous energy and broad group methods. These capabilities have been improved to remove current memory restrictions on the number of samples in continuous energy fixed source calculations and to allow the calculation of fission rates in a tally mesh in broad group fixed source calculations. With these improvements MONK11A can perform fixed source calculations using BINGO point energy data, DICE hyperfine group data or WIMS 172 group data and, in all cases, tally fluxes and reactions in user-defined tally meshes. These tally meshes can be formed from subdivided bodies such as cuboids, cylinders, spheres, or sector bodies. Any number of meshes can be defined, they are independent of each other, and can be independent of the underlying geometry. Each mesh can use its own user-defined energy group scheme for scoring.

Additional options have been added to allow the tallied event counts to be divided by the volumes of the mesh cells in which they are tallied (giving the average number of events per unit volume) and by the number of source particles (giving the average number of events per source neutron). These options can be used together to give the average number of events per source neutron per unit volume.

An example is given in Figure 4 which shows the MONK geometry for LEU-COMP-THERM-048 [9] and the fission density (average number of fissions per source neutron per unit volume) in

a 15x15x10 Cartesian mesh with a single energy group from 0 to 20 MeV. In this case the water height, as shown by the translucent box in the left-hand figure, was adjusted to give a k-eigenvalue of 0.99. Fixed source particles were sampled uniformly in the fuel material with a ^{235}U fission spectrum.

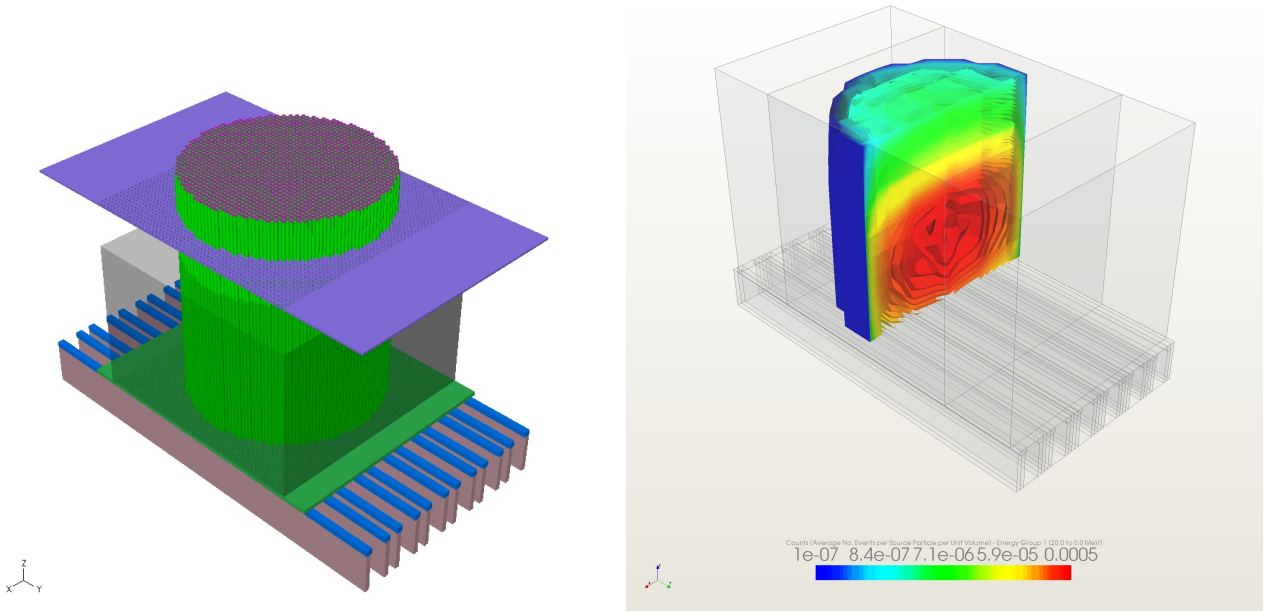

Figure 4: MONK model of LEU-COMP-THERM-048, with water reflector omitted (left), and fission density in a fixed source calculation with a k-eigenvalue of 0.99 (right).

2.4. Improved Parallelization

Current versions of MONK support parallel computation using Open MPI with a master-slave algorithm. It is also possible to run individual loops of a looping calculation concurrently on separate processors. It is currently expected that MONK11A will additionally feature some form of shared memory parallelism and/or tally decomposition, largely aimed at reducing the memory requirements for parallel burn-up calculations.

2.5. Nuclear Data Enhancements

MONK is supplied with data libraries in BINGO point energy, DICE hyperfine group and WIMS broad group formats. Although DICE format libraries are no longer produced for new evaluations each MONK release is accompanied by the latest evaluations in BINGO and WIMS formats. For MONK11A these will be JEFF-3.3 and ENDF/B-VIII.0, in addition to still supporting previous JEFF and ENDF/B evaluations, CENDL3.1 and JENDL3.2.

MONK is able to perform run-time Doppler broadening to any required temperature between the lowest and highest temperatures at which data is tabulated on the supplied BINGO nuclear data library. Currently production-status releases of BINGO libraries have a base temperature of 293.6 K. Recent developments have resulted in the generation of a BINGO library with a base temperature

of 193 K to facilitate below room temperature calculations. This used the validated methodologies and tools which are used to generate production-status BINGO nuclear data libraries.

This new library is based on the nuclear data evaluations in the production-status JEFF-3.1.2 BINGO library, which has been validated for use with MONK10B at 293.6 K. Additional bound thermal scattering data were sourced for hydrogen in ice, hydrogen in polythene and oxygen in ice from the recently published ENDF/B-VIII nuclear data evaluation. Bound scattering data for hydrogen in water at 273.15 K as well as carbon in graphite and hydrogen in zirconium hydride down to 193 K were derived from the experimentally-derived data that underpin the bound scattering data in the production-status JEFF-3.1.2 BINGO library. This library has undergone a verification process to ensure the processed data are correct and provides physically-reasonable results from MONK calculations.

In MONK, each defined material has a temperature associated with it, although this does not have to be explicitly defined and defaults to room temperature (specifically 293.6 K). The BINGO nuclear data library contains cross-section data for each nuclide which have been Doppler broadened to a series of discrete temperatures. For current production status BINGO libraries these temperatures are: 293.6 K, 500 K, 1000 K, 1500 K, 2000 K, 3500 K, 5000 K, 10,000 K, 20,000 K, 40,000 K and 80,000 K. For nuclides present in any material whose temperature is within 0.5 K of one of these library temperatures MONK will use these pre-broadened cross-section data. For any other temperature the BINGO collision processor in MONK10A and later will use run-time Doppler broadening (also known as on-the-fly Doppler broadening) to broaden the resonances to the exact temperature required.

No special user input or expert judgement is required to utilize the run-time Doppler broadening capability in MONK. All that is necessary is for the user to define the temperature of each material, and use a recent BINGO nuclear data library (JEFF-3.1 or later).

The full Doppler broadening treatment as performed by NJOY-BROADR can be computationally expensive for nuclides with complex resonance structures so is not practical to perform during the MONK calculation. Instead BINGO employs an approximate broadening methodology. This method introduces cumulative errors which increase as the temperature moves further away from a tabulated library temperature. For this reason, the BINGO library must contain Doppler broadened (by NJOY-BROADR) cross-section data at a sufficient number of tabulated temperatures to ensure that the approximate broadening method remains sufficiently accurate.

The run-time Doppler broadening method is used in the resolved resonance range for all nuclides. However, it is not suitable for use where the BINGO unresolved resonance subgroup treatment is used in the unresolved resonance range or where bound thermal scattering data are used (see Section 2.3.1). For so-called subgroup nuclides the BINGO library contains subgroup data at a range of intermediate temperatures to allow for interpolation with minimal error.

3. VALIDATION

Validation evidence is of the utmost importance for a code like MONK, and this is provided by the MONK Validation Database which contains over 800 experimental configurations covering a wide range of fissile systems. Each of the benchmarks is run with all of the nuclear data libraries supplied

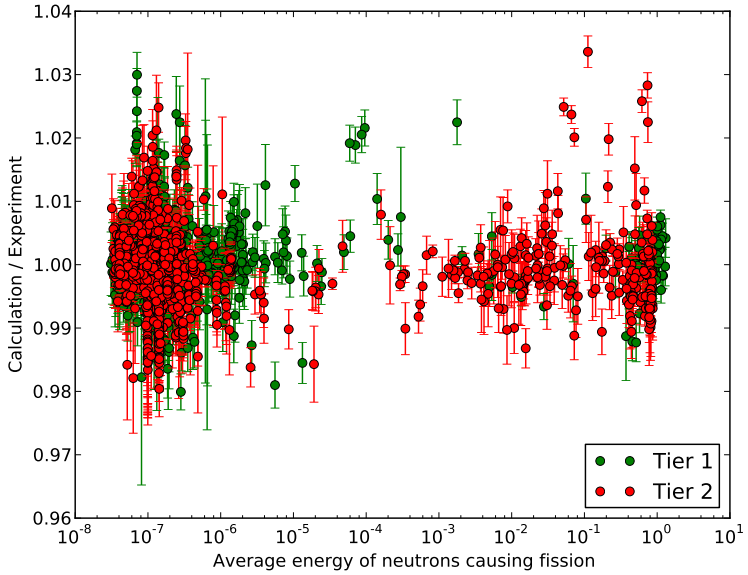

Figure 5: Calculation/Experiment results for the Tier 1 and Tier 2 validation benchmarks plotted against the logarithmic average energy of neutrons causing fission. Error bars show the combined experimental and calculation uncertainty.

with the code before each code release, and verified results are provided to code users. Each of the benchmarks in the MONK Validation Database has to go through a rigorous, independent peer-review process, making it relatively expensive and time consuming to add new benchmarks to the database. For these reasons a second tier of validation benchmarks has been introduced. These have not yet been through the full peer-review process to become full Tier 1 validation cases but have been self-checked and can provide very useful additional validation evidence. Those Tier 2 validation benchmarks which are most applicable to current user validation requirements will be targetted for elevation to Tier 1 status.

A small number of the Tier 1 validation cases are normally excluded due to concerns over the analyses of the experiments, leaving 801 configurations forming the core of the Tier 1 validation set. To these we have so far added 1065 Tier 2 validation cases, all from the ICSBEP Handbook [9], more than doubling the available validation benchmarks and taking the total to 1866 experimental configurations. Figure 5 shows the results for the Tier 1 and Tier 2 validation benchmarks using the JEFF-3.1.2 BINGO nuclear data library. In this figure the Tier 1 results have been generated using the current MONK10B release, while the Tier 2 results have been produced using the development version of MONK11A.

The KRITZ experiments, KRITZ-LWR-RESR-001 to KRITZ-LWR-RESR-003 [10,11,12], which include temperatures up to 248.5°C, have also been added to the Tier 1 benchmarks and will form part of the validation evidence for MONK11A

ACKNOWLEDGEMENTS

The authors gratefully acknowledge the support of EDF Energy, the UK Ministry of Defence, Rolls-Royce, the National Nuclear Laboratory, and the UK Office for Nuclear Regulation.

REFERENCES

[1] S. D. Richards, C. M. J. Baker, P. Cowan, N. Davies, and G. P. Dobson. "MONK and MCBEND: Current Status and Recent Developments." *Annals of Nuclear Energy*, **volume 82**, pp. 63–73 (2015).

[2] S. D. Richards, M. Shepherd, A. Bird, D. Long, C. Murphy, and T. Fry. "Recent Developments to MONK for Criticality Safety and Burnup Credit Applications." In *Proceedings of International Conference on Mathematics and Computational Methods Applied to Nuclear Science and Engineering*. Jeju, South Korea (2017).

[3] E. Woodcock, T. Murphy, P. Hemmings, and S. Longworth. "Techniques used in the GEM Code for Monte Carlo Neutronics Calculation." In *Proceedings of Conference on the Applications of Computing Methods to Reactor Problems*, ANL-7050, pp. 557–579.

[4] E. M. Herman and A. Trkov. *ENDF-6 Formats Manual - Data Formats and Procedures for the Evaluated Nuclear Data Files ENDF/B-VI and ENDF/B-VII*. National Nuclear Data Center, Brookhaven National Laboratory (2010). CSEWG Document ENDF-102, Report BNL-90365-2009 Rev. 1.

[5] L. Snoj and M. Ravnik. "Calculation of Power Density with MCNP in TRIGA reactor." In *International Conference Nuclear Energy for New Europe 2006* (2006).

[6] Y. Nauchi and T. Kameyama. "Development of Calculation Technique for Iterated Fission Probability and Reactor Kinetic Parameters Using Continuous-Energy Monte Carlo Method." *Journal of Nuclear Science and Technology*, **volume 47**, pp. 977–990 (2010).

[7] G. Truchet, P. Leconte, Y. Peneliau, A. Santamarina, and F. Malvagi. "Continuous-Energy Adjoint Flux and Perturbation Calculation usingg the Iterated Fission Probability Method in Monte Carlo Code TRIPOLI-4 and Underlying Applications." In *Proceedings, Joint International Conference on Supercomputing in Nuclear Applications and Monte Carlo*. Paris, France (2013).

[8] S. A. H. Feghhi, M. Shahriari, and H. Afaraideh. "Calculation of Neutron Importance Function in Fissionable Assemblies using Monte Carlo Method." *Annals of Nuclear Energy*, **volume 34**, pp. 514–520 (2007).

[9] NEA Nuclear Science Committee. *International Handbook of Evaluated Criticality Safety Benchmark Experiments* (2018). NEA-1486/16.

[10] L. Snoj, J. C. Gehin, and I. Remec. "KRITZ-2:19 Experiment on Regular H2O/Fuel Pin Lattices with Mixed Oxide Fuel at Temperatures 21.1 and 235.9°C." (2009). KRITZ-LWR-RESR-001.

[11] L. Snoj, J. C. Gehin, and I. Remec. "KRITZ-2:1 Experiment on Regular H2O/Fuel Pin Lattices with Low Enriched Uranium Fuel at Temperatures 248.5°C." (2009). KRITZ-LWR-RESR-002.

[12] L. Snoj, J. C. Gehin, and I. Remec. "KRITZ-2:13 Experiment on Regular H2O/Fuel Pin Lattices with Low Enriched Uranium Fuel at Temperatures 243°C." (2009). KRITZ-LWR-RESR-003.